Hindawi
Advances in Civil Engineering
Volume 2022, Article ID 3675169, 10 pages
https://doi.org/10.1155/2022/3675169

Research Article

Groundwater Risk Assessment of a Rock Cave Type Landfill with Nontraditional Solid Waste

Chenchen Huo,[1] Lijie Guo ,[2,3] Weifang Wu,[1] Runsheng Yang,[1] Yue Zhao ,[2,3] Mingxin Lei,[1] Linfeng Shi,[1] and Baomin Yu[1]

[1]*The Fourth Research and Design Engineering Corporation, CNNC, Shijiazhuang 050021, China*
[2]*Beijing General Research Institute of Mining and Metallurgy, Beijing 100160, China*
[3]*National Centre for International Research on Green Metal Mining, Beijing 102628, China*

Correspondence should be addressed to Lijie Guo; guolijie@bgrimm.com

Received 4 December 2021; Accepted 25 March 2022; Published 27 April 2022

Academic Editor: Bang Yeon Lee

Rock cave landfill has the characteristics of superior geological conditions and strong risk controllability. In this study, taking the first rock cave type nontraditional solid waste landfill in a uranium mine in China as an example, combined with the hydrogeological conditions and engineering characteristics of the mining area, the solute transport model of underground water in a rock cave type nontraditional solid waste landfill was constructed, and the characteristic pollutants were identified, and the pollution migration law of total chromium in the impervious barrier with damaged holes was simulated and characterized. The results show that the leakage of pollutants will affect the groundwater environment when the impervious barrier of the landfill is damaged. The pollution plume exceeding the standard is mainly concentrated in the groundwater aquifer within the landfill area, which is less likely to spread to the off-site environment. The vertical high concentration pollution plume is primarily distributed in the landfill layer. According to the characteristics of rock cave landfills, it is suggested that hazardous solid waste should be separated from surrounding rock. The research results can provide technical guidance for groundwater environment prediction and prevention measures for the same type of project.

1. Introduction

With the continuous advancement of urbanization and industrialization, hazardous waste (HW) production in China continues to overgrow. Industrial nontraditional solid waste is the main source of HW for most cities and regions of China [1, 2]. According to the annual report of environmental statistics 2016–2019, the production and comprehensive utilization and disposal of industrial nontraditional solid waste increased year by year, from 52.195 million tons and 43.172 million tons in 2016 to 81.26 million tons and 75.393 million tons in 2019, up 55.7% and 74.6%, respectively (National Statistical Bulletin on Ecological Environment of 2016–2019, 2020). Industrial nontraditional solid waste has the characteristics of corrosivity, toxicity, flammability, reactivity, and infectivity. It has a wide range of sources and complex components [3–5]. HW has become a critical environmental issue throughout the world [6–8]. Improper disposal of nontraditional solid waste will pose a potential hazard to the atmospheric environment, soil environment, and water resources [9]. The disposal technique for nontraditional solid waste includes comprehensive utilization, incineration, and safe landfill, among which the safe landfill of nontraditional solid waste is the final disposal method of hazardous waste [10].

At present, nontraditional solid waste landfills in China are generally disposed of with surface landfills, and rock cave nontraditional solid waste landfills are the first in China. The rock cave type nontraditional solid waste landfill site has complete and hard surrounding rock as the external natural barrier for nontraditional solid waste disposal. The waste disposal will be less affected by rainfall, temperature, and humidity changes, which reduces the possibility of leachate generation and is convenient for all-round monitoring and

maintenance of the landfill chamber. The environmental risk of nontraditional solid waste landfills was mainly reflected in the leakage of the impervious layer [11]. The groundwater pollution caused by the leakage of leachate caused by the damage to the impermeable layer has become the primary problem of environmental risk of nontraditional solid waste landfills and its surrounding areas [12–14]. However, risk assessment and characterization of groundwater contamination due to rock cave landfills with the seepage of the impervious layer in China have not been studied.

Numerical models are effective means to solve many environmental problems. Models that predict groundwater dynamics can calculate the migration path and concentration trend of pollutants in the environment by generalizing hydrogeological and boundary conditions. Sathe and Mahanta [15] applied MODFLOW to reveal the distribution of arsenic in the aquifer. Tomiyama and others [16] used a numerical model to elucidate the groundwater flow patterns in the abandoned mine area. Huan and others [17] calculated the groundwater nitrate pollution risk based on the modeling method.

The objective of this study was to characterize the spatiotemporal trend of groundwater pollution arising from the condition of damage and continuous leakage of the impervious layer of the first rock cave type nontraditional solid waste landfill of a uranium mine in China. This study provides a basis for the implementation of groundwater environmental protection engineering measures in the landfill site.

2. Research Areas

2.1. Nontraditional Solid Waste. The rock cave type nontraditional solid waste landfill of a uranium mine is filled with HW18 (fly ash and incineration residue) according to the National Catalogue of Hazardous Wastes (NCHWs, hazardous waste list in China). The landfill scale of the underground landfill is 20000 tons per year of fly ash solidified body and 20775 tons per year of incineration residue solidified body. The production service life is 11 years, of which the first year is the capital construction period.

2.2. Physical Geography. The research areas were located in the low mountains and hills in Quzhou City, Zhejiang Province. The central location of the site is 28°50′40″ N and 118°58′36″ E. The altitude of the research areas is 160m ~ 600m, and the terrain of this area is high in the south and low in the north. The terrain of this area fluctuates wildly and is covered with well-developed plants. This area belongs to a subtropical monsoon climate with a humid climate and abundant rainfall. The annual average rainfall is 1763.7 mm, the annual evaporation is 986.5 mm, the yearly average temperature is 17.3°C, the maximum temperature is 40.5°C, and the minimum temperature is -10.4°C.

2.3. The Landscape of Research Areas. To establish the hydrogeological conceptual model for the research areas, field investigation and exploratory drilling were used to obtain the structural information about the aquifer. The hydrogeological information for the site is shown in Figure 1.

The strata in the site area are mainly Quaternary strata and volcanic rocks and pyroclastic rocks of the Upper Jurassic Moshanshi Formation. Quaternary strata are mainly artificial fill and residual slope deposits with small thicknesses. Volcanic rocks and pyroclastic rocks are mainly rhyolite and have a small amount of green layer. The geostructure of the site is located at the junction of the Yangtze Huaihe platform and the South China fold system. The regional structure is mainly NE trending faults, including Jiangshan-Shaoxing deep fault and Datangdi fault. The site mainly develops NNE formation and NWW formation faults (Figure 2), with a fault extension length of 280m ~ 2200m and a width of 1m ~ 20m. Breccia and fracture zones are mostly developed in the fault and filled with siliceous, fault gouge, or kaolin.

2.4. Hydrogeology. The east and west boundary of the research areas are Tongzikeng and Xiaoqiuyuan Rivers, respectively, and the surface water flows from south to north. Groundwater in the site can be divided into Quaternary pore phreatic water, bedrock weathering fissure phreatic water, bedrock fissure water, and structural fissure water. The Quaternary pore phreatic water is the pore water of alluvium and eluvium and the pore water of diluvium. The pore water of alluvium and eluvium is mainly distributed in bands along the Xiaoqiuyuan River. The pore water of diluvium is widely distributed in and around the site, and the thickness of diluvium is 0.5m–5.0 m.

Bedrock weathered fissure phreatic water mainly occurs in strongly weathered bedrock, exposed at the foot of the mountain, low-lying places, and scarps. It is often mixed with pore phreatic water of Quaternary eluvium and diluvium to form a phreatic aquifer with a unified groundwater level. The slightly (non)weathered bedrock is a good impermeable layer.

Bedrock fissure water is mainly distributed in the structural fracture zone or joint fissure dense zone of rock mass caused by multiple tectonic movements, with uneven water distribution and flow of 0.05 L/s ~ 0.62 L/s. Structural fissure water occurs in the structural fissure water-bearing zone. The main structural fissure water-bearing zones in the site are F1, F4, F6, Bailey, and Dachayuan fault-bearing zones, mostly water-blocking faults.

Atmospheric precipitation is the main recharge source of phreatic water in the site area. The phreatic water runoff path is short and has the characteristics of local recharge and discharge. The groundwater flows follow the nature of the terrain to the bottom of the valley and are mainly exposed to the surface in descending springs.

3. Methodology

3.1. Hydrogeological Conceptual Model. Based on the regional hydrogeological conditions in the landfill site and the distribution of sensitive areas, the simulation range is determined as

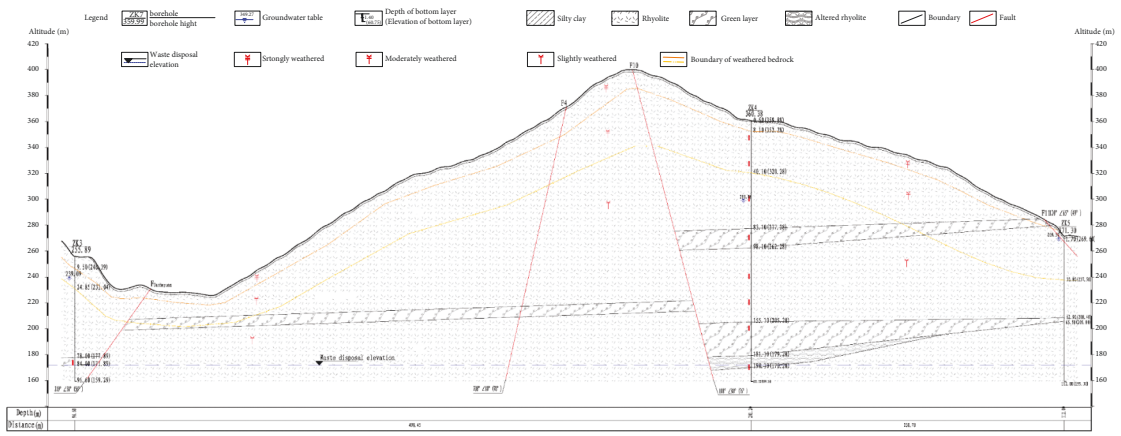

Figure 1: The exploration profiles of the site.

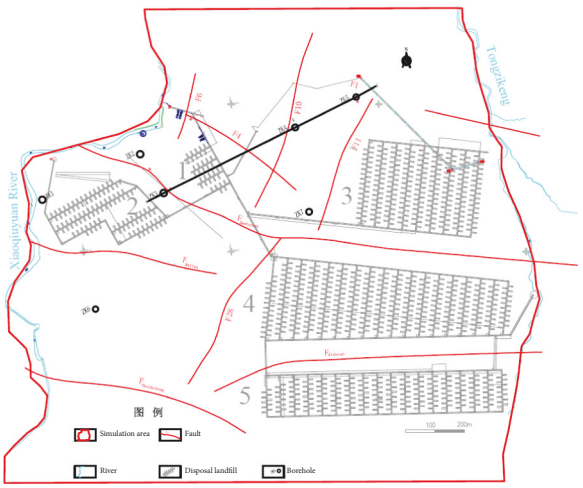

Figure 2: Map of simulation range.

follows: the west is bounded by Xiaoqiuyuan River, the east is bounded by Tongzikeng stream, and the north and south are artificially delineated. The north range is about 300m away from the center of the F1 fault, and the south range is about 310m away from the Shuiduikeng fault. The total area of the simulation area is about 2.4 km^2, which constitutes a relatively complete hydrogeological unit (Figure 2).

According to the information collected from exploratory boreholes and field investigation, the Quaternary eluvium and diluvium are mainly distributed on the two wings of ridge and hillside, with small thickness. Volcanic rocks and pyroclastic rocks are mostly strongly weathered, moderately weathered, and slightly (non)weathered rhyolites. As the rock cave landfill is underground, the design elevation of the landfill area is 170m ~ 185m, and the design elevation is mainly slightly (non)weathered rhyolite. Therefore, to better study the vertical variation of leachate concentration of nontraditional solid waste, the structure stratum can be vertically divided into three layers. The first layer is from the quaternary system to the top plate of the landfill area (185m elevation), the second layer is the location of the landfill layer, 170m ~ 185m, and the third layer is from the bottom plate of the landfill layer to 110m elevations.

The groundwater in the aquifers is conceptualized to be unsteady three dimensional. The aquifers are considered heterogeneous and anisotropic.

The study area is hilly, and the terrain is generally high in the south and low in the north. The groundwater flow direction is consistent with the terrain. Therefore, the southern boundary of the study area is generalized as the second type of constant flow supply boundary, the northern boundary is generalized as the second type of constant flow discharge boundary, and the east and west sides are generalized as the common head boundary. Moreover, the upper boundary is the precipitation supply and evaporation discharge boundary of water, and the lower boundary takes the bedrock as the bottom relative water barrier boundary.

3.2. Boundary Conditions and Pollution Source Settings. Boundary conditions reflect the water and material exchange process and intensity between the model and external system, and reasonable boundary conditions ensure a true reflection of the physical model [18]. The boundary of the model is characterized by local topography and adjacent water bodies. Therefore, the boundary settings were as follows. As the terrain is generally high in the south and low in the north, the south side of the simulation area was set as the second type of constant flow supply boundary. The north side was the discharge boundary of the simulation area. The east and west river are generalized as the common head boundary. The precipitation supply and evaporation discharge boundary is the upper boundary, and the lower boundary takes the bedrock as the bottom relative water barrier boundary. The model domain (including the boundary conditions and positions of the observation wells) is shown in Figure 2.

The landfill site comprises a landfill chamber, landfill roadway, development and transportation roadway, leachate collection tank, groundwater, and an excavation water inflow storage tank, which are successively divided into zone 1 ~ zone 5 (Figure 2). According to the "Standard for pollution control on the hazardous waste landfill" [19], the landfill adopts a rigid antiseepage structure composed of reinforced concrete shell and flexible artificial lining. From bottom to top, it is rock base, antiseepage reinforced concrete,

concrete slope making layer, observation layer, composite geonet, protective layer geotextile, HDPE antiseepage layer, protective layer geotextile, leachate diversion layer pebble, etc. The intact impervious membrane can play a good role in preventing the pollutants in the leachate. However, in the process of nontraditional solid waste disposal and the operation conditions of the landfill, the impervious layer will inevitably be damaged by puncture, tension crack, and aging, resulting in round hole type and crack type damage. The waterproof effect of the damaged impervious structure on the pollutants will be significantly weakened, which is prone to groundwater pollution risk [20].

According to the investigation results of landfill vulnerability density in China and relevant cases [21], it is determined that the vulnerability density of the impervious layer is 30 holes per 4047 m^2, and each hole is a circular hole with a diameter of 10 cm. The leachate flows into the groundwater through the damaged hole is calculated with

$$Q = K * J * A, \tag{1}$$

where Q is the seepage flow at the damaged hole in unit time (m^3/d); K represents the values of hydraulic conductivity of geotextile (m/d); A is the leakage area of the hole(m^2); J is the vertical upward hydraulic gradient.

The hydraulic conductivity of geotextile is 1×10^{-4}~10^{-3} cm/s. To estimate the extreme conditions, the hydraulic conductivity is defined as 1×10^{-3} cm/s, $J = 1.0$. The leakage area is calculated according to the hole with a diameter of 10 cm, and the single hole leachate flow is Q single hole = 0.0067 m^3/d. According to the area of the landfill chamber and landfill roadway in each landfill area, the area where the impervious layer may be damaged is estimated. The leachate flow in each area is as follows: Q Zone 1 = 0.16 m^3/d, Q Zone 2 = 0.62 m^3/d, zone Q Zone 3 = 1.53 m^3/d, Q Zone 4 = 3.21 m^3/d, and Q Zone 5 = 1.37 m^3/d, which are added into the model in the form of the point source.

The solid waste in the landfill site is enriched with $Cr6^+$, Total Cr, Hg, Cd, As, Pb, Ni, and other heavy metal elements. The identification of prediction factors is shown in Table 1. Control limits for entering landfill areas are taken from "Standard for pollution control on the hazardous waste landfill"

3.3. Mathematical Model of Flow and Mass Transport. A commercial professional software developed by Canadian Waterloo Hydrogeologic Inc—Visual MODFLOW—was used in this study to estimate groundwater pollution transportation. The software establishes the groundwater flow model by using the application module for three-dimensional finite-difference numerical simulation [23, 24]. According to the above hydrogeological conceptual model, the groundwater seepage mathematical model in the study area is established in

$$\begin{cases} \dfrac{\partial}{\partial \mathbf{x}}\left(\mathbf{K}\dfrac{\partial \mathbf{H}}{\partial \mathbf{x}}\right) + \dfrac{\partial}{\partial \mathbf{y}}\left(\mathbf{K}\dfrac{\partial \mathbf{H}}{\partial \mathbf{y}}\right) + \dfrac{\partial}{\partial \mathbf{z}}\left(\mathbf{K}\dfrac{\partial \mathbf{H}}{\partial \mathbf{z}}\right) + W = \mu\dfrac{\partial \mathbf{H}}{\partial \mathbf{t}} & (\mathbf{x},\mathbf{y},\mathbf{z})\epsilon\Omega, t > 0, \\ H(\mathbf{x},\mathbf{y},\mathbf{z},\mathbf{t}) = \mathbf{H}_0(\mathbf{x},\mathbf{y},\mathbf{z}) & (\mathbf{x},\mathbf{y},\mathbf{z})\epsilon\Omega, \\ -KM\dfrac{\partial \mathbf{H}}{\partial \mathbf{n}}|\Gamma_2 = q & t > 0, \end{cases} \tag{2}$$

where H_0 is the initial head (m); H is the underground water level elevation (m); K represents the values of hydraulic conductivity (m/d); μ is specific yield; M is the aquifer thickness (m); x, y, and z are the coordinate variables (m); W is vertical water exchange intensity (m^3/d·m^2); q is the unit width seepage flow on the second type of boundary (m^2/d); n is normal direction outside the second type of boundary; Γ_2 is the second type of boundary; and O is the range of calculation area.

Based on the MT3DMS solute transport module, the pollutant transport law of the characteristic pollutant was simulated and predicted under the condition of continuous leakage. In this study, the adsorption and chemical reaction terms are not considered. Only the convection dispersion effect is considered, and the pollutant transport simulation is carried out based on the groundwater flow numerical model. The solute transport equation used in this simulation is

$$\begin{cases} n\dfrac{\partial \mathbf{C}}{\partial \mathbf{t}} = \dfrac{\partial}{\partial \mathbf{x_i}}\left(\mathbf{n}\mathbf{D_{ij}}\dfrac{\partial \mathbf{C}}{\partial \mathbf{x_i}}\right) - \dfrac{\partial}{\partial \mathbf{x_i}}(\mathbf{n}\mathbf{v_i}\mathbf{C}) + \mathbf{q_s}\mathbf{C_s}\ (\mathbf{x},\mathbf{y},\mathbf{z}) \in \Omega,\ i, j = 1, 2, 3,\ t > 0, \\ C(\mathbf{x},\mathbf{y},\mathbf{z},0) = \mathbf{C}_0(\mathbf{x},\mathbf{y},\mathbf{z}) \qquad (\mathbf{x},\mathbf{y},\mathbf{z}) \in \Omega, t = 0, \end{cases} \tag{3}$$

Table 1: Predictor identification.

Item	Cr6+	Total Cr	Hg	Cd	As	*P*b	Ni
Control limit for entering landfill area (mg/L)	6	15	0.12	0.6	2	1.2	2
Class III standard	0.05	0.05	0.001	0.005	0.01	0.01	0.02
Standard index	120	300	120	120	200	120	100

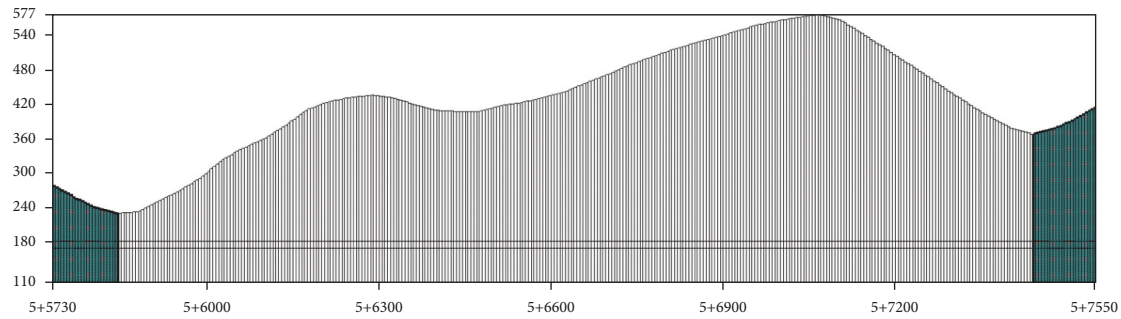

Figure 3: Vertical section of the grid.

where n is the medium porosity; C is the mass fraction of component ($mg \cdot L^{-1}$); t is the time; Dij is the hydrodynamic dispersion coefficient tensor ($m^2 \cdot d^{-1}$); Vi is the groundwater seepage velocity tensor ($m \cdot d^{-1}$); O is the calculation area; C_0 is the initial mass fraction distribution ($mg \cdot L^{-1}$); qs is the volume flow of source and sink of unit volume aquifer; Cs is the mass fraction of components in source and sink water ($mg \cdot L^{-1}$).

3.4. Model Construction and Calibration. Rectangular grids of 5m × 5m were used to subdivide the modelled area. The whole simulation area is divided into 324 rows along the north-south direction and 364 columns along the east-west direction. There are 97455 effective cells, representing the actual area of 2.4 km2. Vertically, the whole simulation area is divided into three layers, and the calculation area is divided into 292365 active units in space. Figure 3 shows the vertical section of the grid. The 1 : 2000 topographic map in the study area is digitised to form elevation data. After elevation points are extracted, and abnormal points are eliminated, the original elevation data of the simulation area are obtained. On this basis, the Kriging spatial interpolation method is further used to generate the digital elevation model [25], which meets the accuracy requirements of establishing the groundwater flow numerical model (Figure 4).

The main factors controlling the accuracy of the model predictions were hydrogeological parameters and solute transport parameters, which were obtained by in situ hydrogeological experiments and similar lithology investigation data. The values of various parameters for the reasonable-fit model are shown in Table 2, including the values of hydraulic conductivities (K) and the water yield of each layer.

The model was calibrated to enhance simulation reliability. A manual trial-and-error calibration method was used to achieve the calibration. The predicted output flow field was compared with the measured water level data to verify the rationality of the model [26–28]. The smaller the value of the standard error of the estimate, the closer the model predictions were to the actual observation values, and the higher the model accuracy. Seven hydrogeological boreholes in the area are used for identification and correction. The results are shown in Figure 5. Figure 6 shows that the correlation coefficient of water level fitting is 0.998, proving that the fitting effect is good. After the model identification, the initial groundwater flow field in the study area is obtained, as shown in Figure 7.

4. Results and Discussion

According to the design life of the landfill, the characteristic pollutant transport of the landfill in 20 years is simulated. Figure 8 and Figure 9 show the migration and diffusion of total chromium in the landfill's groundwater after the first, fifth, tenth, and twentieth years. Table 3 lists the simulation results of pollution plume migration distance and pollution area of total chromium at the above time points.

After the first year, five years, ten years, and twenty years, the predicted maximum concentration of total chromium was 0.2 mg/l, 0.45 mg/l, 0.6 mg/l, and 0.8 mg/l, respectively, under the condition of continuous leakage of pollutants, and no prevention measures were taken, exceeding the requirements of class III standard limit in groundwater quality standard. The maximum concentration was mainly distributed in the landfill site. On the plane, the pollution plume moves along the flow direction of groundwater as a whole. After the first year, the pollution plume in each landfill area is basically centered on the point source, and the diffusion area is small. From the 5th year to the 20th year, the pollution plume takes the point source as the center, the horizontal migration distance increases, and the area of the pollution plume increases. After 20 years, the pollution plume of the landfills in zone 3, zone 4, and zone 5 passes through the Dachayuan fault and Xishansi fault in the site, and other faults are less affected by pollution. After 20 years

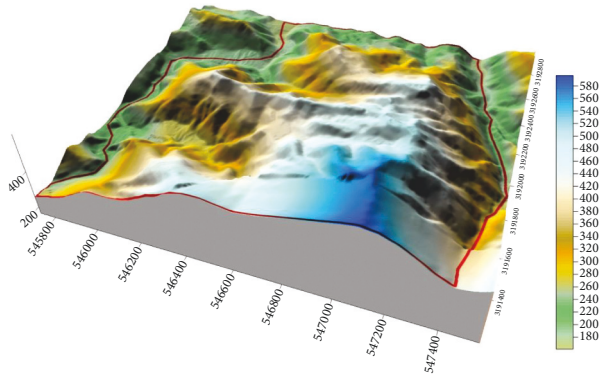

Figure 4: Digital elevation model of the study area.

Table 2: Hydrogeological parameters of the validated groundwater flow model.

Number	Lithology	Kxx/(m/d)	Kyy/(m/d)	Kzz/(m/d)	μ
1	Quaternary	0.2~1	0.2~1	0.2~1	0.2
2	Strongly weathered bedrock	0.1~0.2	0.1~0.2	0.1~0.2	0.1
3	Moderate weathered bedrock	0.02	0.02	0.02	0.05
4	Slightly nonweathered bedrock	0.002~0.02	0.002~0.02	0.002~0.02	0.05
5	Fault	0.0055~0.012	0.0055~0.012	0.0055~0.012	0.05

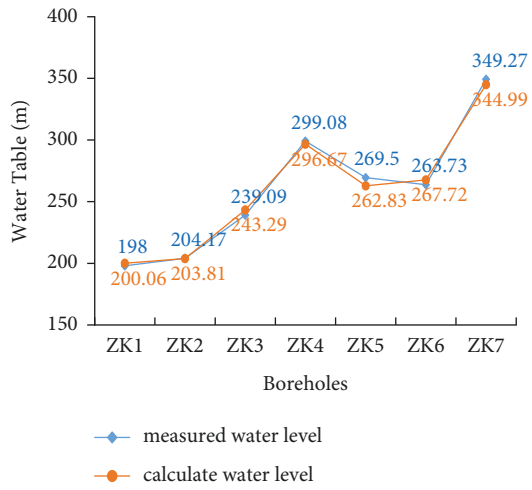

Figure 5: Comparison between calculated water level and measured water level.

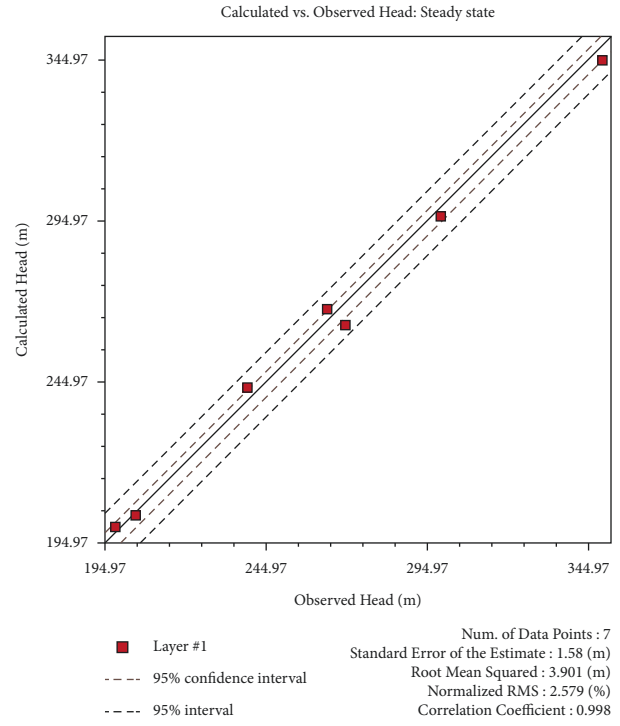

Figure 6: Fitting diagram of calculated water level and measured water level.

of continuous leakage, the areas of groundwater quality exceeding the standard in each landfill area are 0.03m2, 0.07m2, 0.16m2, 0.27m2, and 0.18m2, respectively, and the maximum migration distances from the pollution plume center are 158.48 m, 180.82 m, 253.57 m, 396.20 m, and 419.97 m. During the simulation period, the excessive range of total chromium pollution plume is mainly concentrated in the underground aquifer within the landfill area, the excessive range does not migrate to the surface water, and the leachate has little impact on the groundwater environment around the site.

Vertically, no top waterproof layer is set for nontraditional solid waste in the model, and the leachate is in direct contact with the top and sidewalls of the surrounding rock. Due to convection and dispersion, the damage to the impervious layer will cause pollutants to have a specific impact on the upper and lower aquifers of the landfill layer. Due to the small permeability coefficient of the surrounding rock, the pollutant concentration in the upper and lower aquifers of the landfill layer is low, and the high concentration pollution plume is still mainly distributed in the landfill layer.

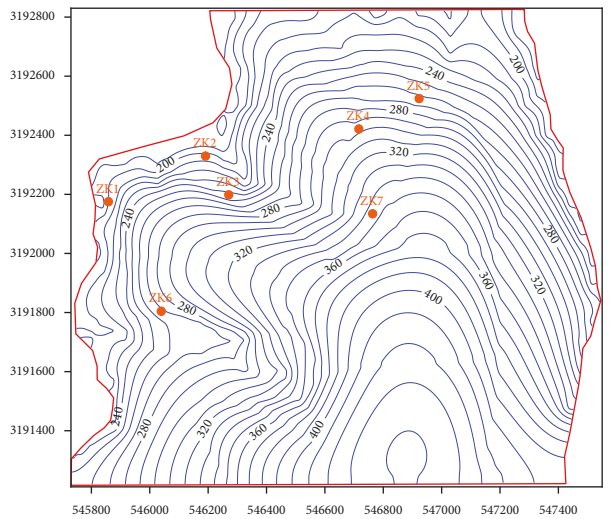

Figure 7: Initial flow field in the simulation area.

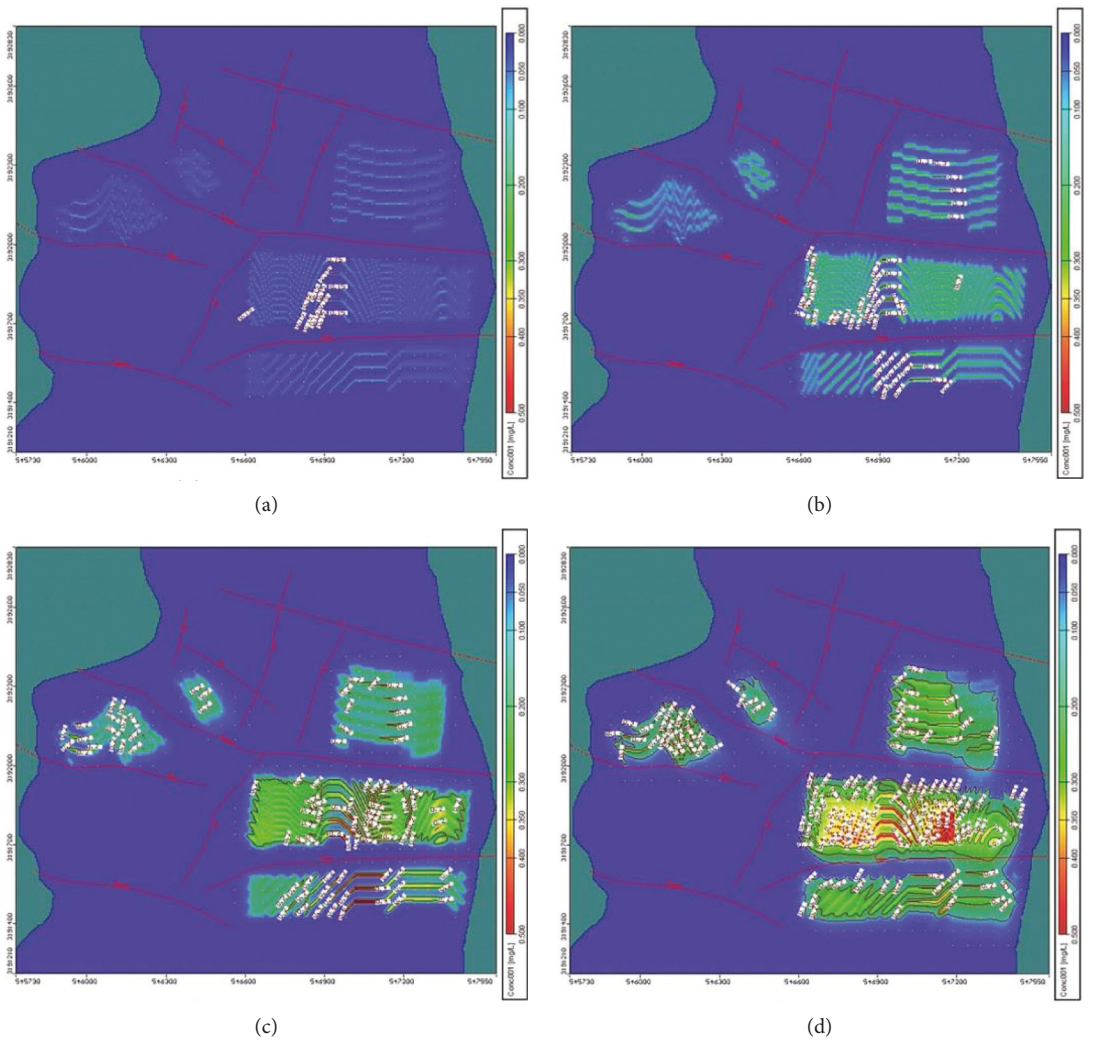

Figure 8: Total chromium pollution plume of disposal layer in the study area.

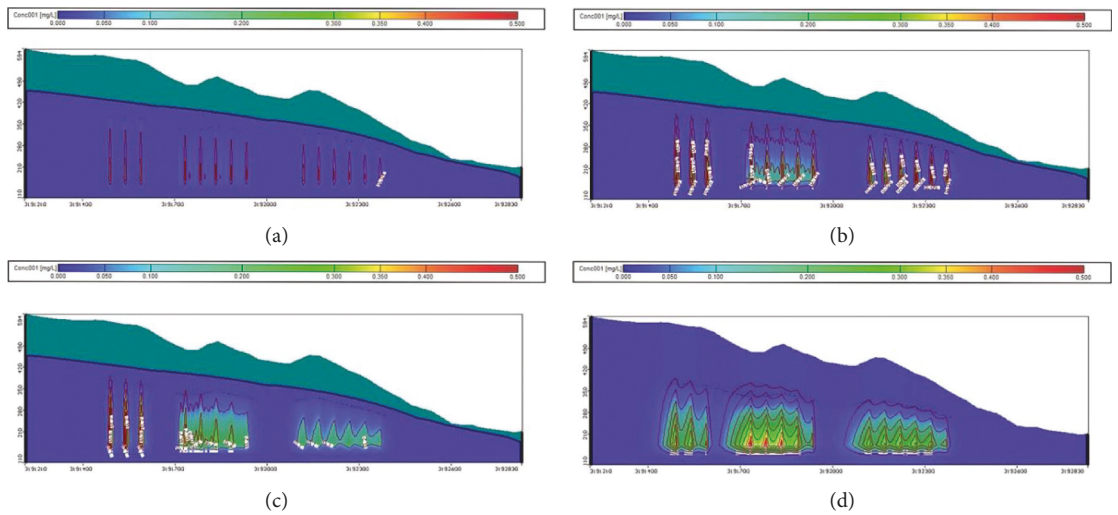

Figure 9: Total chromium pollution plume profile in the study area.

Table 3: Prediction results of total chromium pollution plume in groundwater.

	Zone 1		Zone 2		Zone 3		Zone 4		Zone 5	
	Maximum horizontal migration distance (m)	Polluted area (m2)	Maximum horizontal migration distance (m)	Polluted area (m2)	Maximum horizontal migration distance (m)	Polluted area (m2)	Maximum horizontal migration distance (m)	Polluted area (m2)	Maximum horizontal migration distance (m)	Polluted area (m2)
1 year	0.00	0.00	158.33	0.01	200.00	0.07	366.67	0.10	166.67	0.04
5 year	95.42	0.02	130.17	0.04	213.33	0.12	395.00	0.22	387.50	0.13
10 year	120.50	0.03	137.67	0.065	222.50	0.13	404.17	0.22	416.67	0.14
20 year	158.48	0.03	180.82	0.07	253.57	0.16	396.20	0.27	419.97	0.18

Note. The maximum horizontal migration distance is the maximum horizontal distance from the center of the pollution plume [19]. Taking the maximum value of the standard index, the prediction factor of this simulation is total Cr. According to the landfill scheme, the aquifer with an elevation of 170m ~ 185m is set as the polluted layer. The concentration of leakage pollutants is 15 mg/L. The final migration boundary concentration of pollutants refers to the class III standard limit in the "Standard for groundwater quality" [22].

5. Conclusions and Recommendations

This paper establishes a hydrogeological numerical model for the first cave type nontraditional solid waste landfill in a uranium mine in China, revealing the risk of groundwater pollution under continuous leachate leakage. The results justify the following conclusions.

In the case of continuous leakage of hole pollutant leachate in the impervious layer and no prevention measures are taken, the diffusion range of total chromium pollution gradually expands with time in the simulation period. Due to the slight leakage of pollutants and the small permeability coefficient of the aquifer, combined with the project layout scheme, the excessive range of pollution plume is mainly concentrated in the underground aquifer within the landfill area, the migration distance is short, and the possibility of diffusion to the off-site environment is slight. Therefore, it has little impact on the groundwater environment around the site. Vertically, the high concentration pollution plume is mainly distributed in the landfill layer and has little effect on the upper and lower aquifers of the landfill layer.

During the construction and landfill of the nontraditional solid waste landfill, the construction and landfill shall be carried out in strict accordance with relevant standards and guidelines to ensure the integrity of the impervious layer and reduce the risk of groundwater pollution caused by the damage of the impermeable layer. The rock cave type nontraditional solid waste landfill is still the first case in China. This study proves that it is feasible to use the rock cave type to safely landfill industrial hazardous waste, which has a particular reference significance for the implementation of similar projects in the future.

According to the characteristics of the rock cave type nontraditional solid waste landfill, to reduce the possibility of the impact of pollutants on the groundwater environment, it is recommended to set up space isolation between the solid waste and the chamber wall, such as HDPE waterproof layer on the top and a particular gap between the protective pool and the chamber wall. The patrol inspection and leachate monitoring of the landfill site are strengthened during the landfill and operation period. [29].

Data Availability

Data are available from the corresponding author upon request.

Conflicts of Interest

CH, WW, RY, ML, LS, and BY were employed by the Fourth Research and Design Engineering Corporation. The remaining authors declare that the research was conducted in the absence of any commercial or financial relationships that could be construed as a potential conflict of interest.

Authors' Contributions

CH, LG, and WW contributed to conceptualisation; CH and RY contributed to data curation; CH and ML contributed to formal analysis; LG contributed to funding acquisition; CH and WW contributed to the investigation; CH, WW, LS, and BY contributed to methodology; CH, WW, and BY contributed to numerical modeling; CH contributed to visualisation; CH contributed to writing the original draft; LG, WW, RY, YZ, ML, LS, and BY contributed to review and editing.

Acknowledgments

The authors would also like to thank the Zhejiang Quzhou Industry Corporation of China for their technical support. Financial support from the National Key Research and Development Program of China (2018YFE0123000) is gratefully acknowledged.

References

[1] H. Duan, Q. Huang, Q. Wang, B. Zhou, and J. Li, "Hazardous waste generation and management in China: a review," *Journal of Hazardous Materials*, vol. 158, no. 2-3, pp. 221–227, 2008.

[2] P. Kang, H. Zhang, and H. Duan, "Characterising the implications of waste dumping surrounding the Yangtze River economic belt in China," *Journal of Hazardous Materials*, vol. 383, pp. 121–207, 2020.

[3] A. Augustsson, T. Uddh Söderberg, J. Jarsjö et al., "The risk of overestimating the risk-metal leaching to groundwater near contaminated glass waste deposits and exposure via drinking water," *The Science of the Total Environment*, vol. 566-567, pp. 1420–1431, 2016.

[4] Y. Chen, L. Xu, S. N. Tan, X. Sun, Y. Deng, and W. Yang, "Solidification and multi-cytotoxicity evaluation of thermally treated MSWI fly ash," *Journal of Hazardous Materials*, vol. 388, Article ID 122041, 2020.

[5] M. Guarienti, A. Gianoncelli, E. Bontempi et al., "Biosafe inertization of municipal solid waste incinerator residues by COSMOS technology," *Journal of Hazardous Materials*, vol. 279, pp. 311–321, 2014.

[6] G. Salihoglu, "Industrial hazardous waste management in Turkey: current state of the field and primary challenges," *Journal of Hazardous Materials*, vol. 177, no. 1-3, pp. 42–56, 2010.

[7] K. Orloff and H. Falk, "An international perspective on hazardous waste practices," *International Journal of Hygiene and Environmental Health*, vol. 206, no. 4-5, pp. 291–302, 2003.

[8] L. Fazzo, F. Minichilli, M. Santoro et al., "Hazardous waste and health impact: a systematic review of the scientific literature," *Environmental Health*, vol. 16, no. 1, p. 107, 2017.

[9] V. Misra and S. D. Pandey, "Hazardous waste, impact on health and environment for development of better waste management strategies in future in India," *Environment International*, vol. 31, no. 3, pp. 417–431, 2005.

[10] R. Malviya and R. Chaudhary, "Factors affecting hazardous waste solidification/stabilization: a review," *Journal of Hazardous Materials*, vol. 137, no. 1, pp. 267–276, 2006.

[11] G. Hamer, "Solid waste treatment and disposal: effects on public health and environmental safety," *Biotechnology Advances*, vol. 22, no. 1-2, pp. 71–79, 2003.

[12] T. M. Alslaibi, Y. K. Mogheir, and S. Afifi, "Assessment of groundwater quality due to municipal solid waste landfills leachate," *Journal of Environmental Science and Technology*, vol. 4, no. 4, pp. 419–436, 2011.

[13] S. Banu and T. Berrin, "Parametric fate and transport profiling for selective groundwater monitoring at closed landfills: a case study," *Waste Management Series*, vol. 38, pp. 263–270, 2015.

[14] G. X. Chen, L. Wang, G. C. Wang, and J. H. Liu, "Modeling the transportation of pollutants in shallow groundwater in the landfill site near a medium city," *Hydrogeology & Engineering Geology*, vol. 6, pp. 112–116, 2008.

[15] S. S. Sathe and C. Mahanta, "Groundwater flow and arsenic contamination transport modeling for a multi aquifer terrain: assessment and mitigation strategies," *Journal of Environmental Management*, vol. 231, pp. 166–181, 2019.

[16] S. Tomiyama, T. Igarashi, C. B. Tabelin, P. Tangviroon, and H. Ii, "Modeling of the groundwater flow system in excavated areas of an abandoned mine," *Journal of Contaminant Hydrology*, vol. 230, 2020.

[17] H. Huan, L. Hu, and Y. Yang, "Groundwater nitrate pollution risk assessment of the groundwater source field based on the integrated numerical simulations in the unsaturated zone and saturated aquifer," *Environment International*, vol. 137, Article ID 105532, 2020.

[18] F. Lachaal and S. Gana, "Groundwater flow modeling for impact assessment of port dredging works on coastal hydrogeology in the area of Al-Wakrah (Qatar)," *Modeling Earth Syst. Environ*, vol. 2, 2016.

[19] GB 18598, *Taking the Maximum Value of the Standard index, the Prediction Factor of This Simulation Is Total Chromium*, (In Chinese), Beijing, China, 2019.

[20] L. Zhou, D. An, Y. Yang, B. Xi, and Y. Wang, "Predicting leakage and contaminant transport through composite liners in hazardous waste landfill," *Acta Scientiae Circumstantiae*, vol. 37, no. 6, pp. 2210–2217, 2017, (In Chinese).

[21] Y. Xu, C. Neng, and Y. Liu, "Statistical analysis on density of accidental-hole in landfill liner system," *Chinese Journal of Environmental Engineering*, vol. 9, pp. 4558–4564, 2015.

[22] Gb/T 14848, *Standard for Groundwater Quality*, National Standard Of The People's Republic Of China, Beijing, China, 2017.

[23] S. F. R. Khadri and C. Pande, "Ground water flow modeling for calibrating steady state using MODFLOW software: a case study of Mahesh River basin, India," *Modeling Earth Syst. Environ*, vol. 2, 2016.

[24] W. Li, Y. Y. Zhang, Y. Y. Zhang, X. Li, and C. Shen, "Research on the deep foundation pit dewatering design by three-dimensional numerical simulation," *Urban. Geotech. Investig. Surv*, vol. 1, pp. 189–192, 2019.

[25] T. M. Milillo and J. A. Gardella, "Spatial analysis of time of flight-secondary ion mass spectrometric images by ordinary kriging and inverse distance weighted interpolation techniques," *Analytical Chemistry*, vol. 80, pp. 4896–4905, 2008.

[26] S. Okhravi, S. Eslamian, and N. Fathianpour, "Assessing the effects of flow distribution on the internal hydraulic behavior of a constructed horizontal subsurface flow wetland using a

numerical model and a tracer study," *Ecohydrology and Hydrobiology*, vol. 18, p. 307, 2018.

[27] S. Guo, H. Wu, Y. Tian, H. Chen, Y. Wang, and J. Yang, "Migration and fate of characteristic pollutants migration from an abandoned tannery in soil and groundwater by experiment and numerical simulation," *Chemosphere*, vol. 271, Article ID 129552, 2021.

[28] X. Bai, K. Song, J. Liu, A. K. Mohamed, C. Mou, and D. Liu, "Health risk assessment of groundwater contaminated by oil pollutants based on numerical modeling," *International Journal of Environmental Research and Public Health*, vol. 16, no. 18, p. 3245, 2019.

[29] Ministry of Ecology and Environment of the People's Republic of China, "National statistical bulletin on ecological environment of 2016-2019," 2020, https://www.mee.gov.cn/hjzl/sthjzk/sthjtjnb/.